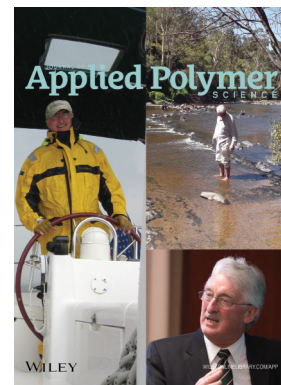


Special Issue: Sustainable Polymers and Polymer Science  
Dedicated to the Life and Work of Richard P. Wool

Guest Editors: Dr Joseph F. Stanzione III (Rowan University, U.S.A.)  
and Dr John J. La Scala (U.S. Army Research Laboratory, U.S.A.)



#### EDITORIAL

Sustainable Polymers and Polymer Science: Dedicated to the Life and Work of Richard P. Wool  
Joseph F. Stanzione III and John J. La Scala, *J. Appl. Polym. Sci.* 2016, DOI: [10.1002/app.44212](https://doi.org/10.1002/app.44212)

#### REVIEWS

Richard P. Wool's contributions to sustainable polymers from 2000 to 2015  
Alexander W. Bassett, John J. La Scala and Joseph F. Stanzione III, *J. Appl. Polym. Sci.* 2016,  
DOI: [10.1002/app.43801](https://doi.org/10.1002/app.43801)

Recent advances in bio-based epoxy resins and bio-based epoxy curing agents  
Elyse A. Baroncini, Santosh Kumar Yadav, Giuseppe R. Palmese and Joseph F. Stanzione III, *J. Appl. Polym. Sci.* 2016,  
DOI: [10.1002/app.44103](https://doi.org/10.1002/app.44103)

Recent advances in carbon fibers derived from bio-based precursors  
Amod A. Ogale, Meng Zhang and Jing Jin, *J. Appl. Polym. Sci.* 2016, DOI: [10.1002/app.43794](https://doi.org/10.1002/app.43794)

#### RESEARCH ARTICLES

Flexible polyurethane foams formulated with polyols derived from waste carbon dioxide  
Mica DeBolt, Alper Kiziltas, Deborah Mielewski, Simon Waddington and Michael J. Nagridge, *J. Appl. Polym. Sci.* 2016,  
DOI: [10.1002/app.44086](https://doi.org/10.1002/app.44086)

Sustainable polyacetals from erythritol and bioaromatics  
Mayra Rostagno, Erik J. Price, Alexander G. Pemba, Ion Ghiriviga, Khalil A. Abboud and Stephen A. Miller, *J. Appl. Polym. Sci.*  
2016, DOI: [10.1002/app.44089](https://doi.org/10.1002/app.44089)

Bio-based plasticizer and thermoset polyesters: A green polymer chemistry approach  
Mathew D. Rowe, Ersan Eyiler and Keisha B. Walters, *J. Appl. Polym. Sci.* 2016, DOI: [10.1002/app.43917](https://doi.org/10.1002/app.43917)

The effect of impurities in reactive diluents prepared from lignin model compounds on the properties of vinyl ester resins  
Alexander W. Bassett, Daniel P. Rogers, Joshua M. Sadler, John J. La Scala, Richard P. Wool and Joseph F. Stanzione III,  
*J. Appl. Polym. Sci.* 2016, DOI: [10.1002/app.43817](https://doi.org/10.1002/app.43817)

Mechanical behaviour of palm oil-based composite foam and its sandwich structure with flax/epoxy composite  
Siew Cheng Teo, Du Ngoc Uy Lan, Pei Leng Teh and Le Quan Ngoc Tran, *J. Appl. Polym. Sci.* 2016, DOI: [10.1002/app.43977](https://doi.org/10.1002/app.43977)

Mechanical properties of composites with chicken feather and glass fibers  
Mingjiang Zhan and Richard P. Wool, *J. Appl. Polym. Sci.* 2016, DOI: [10.1002/app.44013](https://doi.org/10.1002/app.44013)

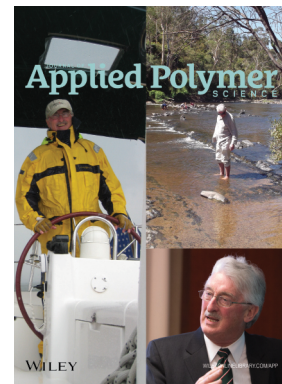
Structure–property relationships of a bio-based reactive diluent in a bio-based epoxy resin  
Anthony Maiorana, Liang Yue, Ica Manas-Zloczower and Richard Gross, *J. Appl. Polym. Sci.* 2016, DOI: [10.1002/app.43635](https://doi.org/10.1002/app.43635)

Bio-based hydrophobic epoxy-amine networks derived from renewable terpenoids  
Michael D. Garrison and Benjamin G. Harvey, *J. Appl. Polym. Sci.* 2016, DOI: [10.1002/app.43621](https://doi.org/10.1002/app.43621)

Dynamic heterogeneity in epoxy networks for protection applications  
Kevin A. Masser, Daniel B. Knorr Jr., Jian H. Yu, Mark D. Hindenlang and Joseph L. Lenhart, *J. Appl. Polym. Sci.* 2016,  
DOI: [10.1002/app.43566](https://doi.org/10.1002/app.43566)

Special Issue: Sustainable Polymers and Polymer Science  
Dedicated to the Life and Work of Richard P. Wool

Guest Editors: Dr Joseph F. Stanzione III (Rowan University, U.S.A.)  
and Dr John J. La Scala (U.S. Army Research Laboratory, U.S.A.)



Statistical analysis of the effects of carbonization parameters on the structure of carbonized electrospun organosolv lignin fibers

Vida Poursorkhabi, Amar K. Mohanty and Manjusri Misra, *J. Appl. Polym. Sci.* 2016, DOI: 10.1002/app.44005

Effect of temperature and concentration of acetylated-lignin solutions on dry-spinning of carbon fiber precursors

Meng Zhang and Amod A. Ogale, *J. Appl. Polym. Sci.* 2016, DOI: 10.1002/app.43663

Poly(lactic acid) bioconjugated with glutathione: Thermosensitive self-healed networks

Dalila Djidi, Nathalie Mignard and Mohamed Taha, *J. Appl. Polym. Sci.* 2016, DOI: 10.1002/app.43436

Sustainable biobased blends from the reactive extrusion of polylactide and acrylonitrile butadiene styrene

Ryan Vadori, Manjusri Misra and Amar K. Mohanty, *J. Appl. Polym. Sci.* 2016, DOI: 10.1002/app.43771

Physical aging and mechanical performance of poly(L-lactide)/ZnO nanocomposites

Erlantz Lizundia, Leyre Pérez-Álvarez, Míriam Sáenz-Pérez, David Patrocínio, José Luis Vilas and Luis Manuel León, *J. Appl. Polym. Sci.* 2016, DOI: 10.1002/app.43619

High surface area carbon black (BP-2000) as a reinforcing agent for poly[(-)-lactide]

Paula A. Delgado, Jacob P. Brutman, Kristina Masica, Joseph Molde, Brandon Wood and Marc A. Hillmyer, *J. Appl. Polym. Sci.* 2016, DOI: 10.1002/app.43926

Encapsulation of hydrophobic or hydrophilic iron oxide nanoparticles into poly-(lactic acid) micro/nanoparticles via adaptable emulsion setup

Anna Song, Shaowen Ji, Joung Sook Hong, Yi Ji, Ankush A. Gokhale and Ilsoon Lee, *J. Appl. Polym. Sci.* 2016, DOI: 10.1002/app.43749

Biorenewable blends of polyamide-4,10 and polyamide-6,10

Christopher S. Moran, Agathe Barthelon, Andrew Pearsall, Vikas Mittal and John R. Dorgan, *J. Appl. Polym. Sci.* 2016, DOI: 10.1002/app.43626

Improvement of the mechanical behavior of bioplastic poly(lactic acid)/polyamide blends by reactive compatibilization

JeongIn Gug and Margaret J. Sobkowicz, *J. Appl. Polym. Sci.* 2016, DOI: 10.1002/app.43350

Effect of ultrafine talc on crystallization and end-use properties of poly(3-hydroxybutyrate-co-3-hydroxyhexanoate)

Jens Vandewijngaarden, Marius Murariu, Philippe Dubois, Robert Carleer, Jan Yperman, Jan D'Haen, Roos Peeters and Mieke Buntinx, *J. Appl. Polym. Sci.* 2016, DOI: 10.1002/app.43808

Microfibrillated cellulose reinforced non-edible starch-based thermoset biocomposites

Namrata V. Patil and Anil N. Netravali, *J. Appl. Polym. Sci.* 2016, DOI: 10.1002/app.43803

Semi-IPN of biopolyurethane, benzyl starch, and cellulose nanofibers: Structure, thermal and mechanical properties

Md Minhaz-Ul Haque and Kristiina Oksman, *J. Appl. Polym. Sci.* 2016, DOI: 10.1002/app.43726

Lignin as a green primary antioxidant for polypropylene

Renan Gadioli, Walter Ruggeri Waldman and Marco Aurelio De Paoli, *J. Appl. Polym. Sci.* 2016, DOI: 10.1002/app.43558

Evaluation of the emulsion copolymerization of vinyl pivalate and methacrylated methyl oleate

Alan Thyago Jensen, Ana Carolina Couto de Oliveira, Sílvia Belém Gonçalves, Rossano Gambetta and Fabricio Machado, *J. Appl. Polym. Sci.* 2016, DOI: 10.1002/app.44129

## Encapsulation of hydrophobic or hydrophilic iron oxide nanoparticles into poly(lactic acid) micro/nanoparticles via adaptable emulsion setup

Anna Song, Shaowen Ji, Joung Sook Hong, Yi Ji, Ankush A. Gokhale, Ilsoon Lee

Department of Chemical Engineering and Materials Science, Michigan State University, East Lansing, Michigan 48824

Correspondence to: I. Lee; (E-mail: leeil@egr.msu.edu)

**ABSTRACT:** In this study, a one-step water-in-oil-in-water (W/O/W) emulsion process was employed to encapsulate either hydrophilic (~10 nm) or hydrophobic (~5 nm) iron oxide nanoparticles (IONPs) into poly(lactic acid) (PLA). Via the simple adjustment of emulsification temperature to high temperature (HT, 60 °C) or room temperature (RT, 25 °C), a transformation of PLA-IONPs composite particles from hollow microparticles to solid nanospheres can be achieved. At RT, PLA nanocomposite particles (30–200 nm) encapsulating IONPs were generated regardless of the hydrophobicity of IONPs. On the other hand, at HT, our method resulted in the hollow microparticles (2–5 μm). This study presents a fast and easily adaptable process to encapsulate either hydrophobic or hydrophilic IONPs into the hydrophobic polymeric particles, with different shapes and sizes, by simply adjusting the emulsification temperature through the one-step W/O/W emulsion. © 2016 Wiley Periodicals, Inc. *J. Appl. Polym. Sci.* **2016**, *133*, 43749.

**KEYWORDS:** applications; biodegradable; composites; magnetic nanoparticles; nanoparticles; poly(lactic acid)

Received 14 January 2016; accepted 7 April 2016

DOI: 10.1002/app.43749

### INTRODUCTION

Magnetic nanoparticles have attracted significant interest across a wide range of research areas, including biomedicine and drug delivery,<sup>1</sup> magnetic resonance imaging (MRI),<sup>2</sup> magnetic fluids,<sup>3</sup> catalysis,<sup>4</sup> and environmental remediation.<sup>5,6</sup> In the biomedical field, magnetic nanoparticles have been used for magnetic targeting delivery. As early as the 1970s, microspheres entrapped with iron oxide were used in targeted cancer therapy by applying a magnetic field.<sup>7,8</sup> Magnetic nanoparticles have also been studied as diagnostic agents to increase image contrast for both *in vivo* and *in vitro* diagnosis, like Magnetic Resonance imaging (MRI) tumor detection.<sup>9</sup>

For successful application of magnetic nanoparticles, it is necessary to overcome several problems associated with particle stability, such as aggregation, undesirable chemical activity, and losses of dispersibility and magnetism.<sup>10</sup> So far, several protection strategies such as coating the magnetic nanoparticles with surfactants and polymers, an inorganic layer such as silica or carbon, and embedding magnetic nanoparticles into a matrix have been developed to prevent the agglomeration and corrosion of naked magnetic nanoparticles.<sup>10</sup> For example, Ferumoxide, an FDA-approved IONP formulation with a size range of 100–150 nm, contains a 5–10 nm IONP core. Similar to other coating methods, it results in a core-shell structure for each magnetic nanoparticle.<sup>11</sup> These individually protected IONPs have good dispersibility, yet low content (around 0.01%) of

IONPs in the whole core-shell particle, which leads to low cell labeling efficiency.<sup>12,13</sup> Compared with this core-shell type of IONPs, direct entrapment of IONPs into a matrix provides a higher loading efficiency. Commercially available micron-sized iron oxide particles (MPIOs, Bangs Laboratories, Fishers, IN) have been developed with around 50 wt % iron oxide content.<sup>14,15</sup> However, current commercialized MPIOs use the inert matrix, polystyrene/divinylbenzene, to encapsulate IONPs, limiting their biomedical applications. Recently, M. K. Nkansah *et al.*<sup>16</sup> reported the use of a biodegradable polymer, poly(lactide-co-glycolide) (PLGA), to encapsulate IONPs for MRI cell tracking. In this study, both micro- and nano-sized magnetic PLGA particles have been prepared to fulfill different applicable requirements.<sup>16</sup> Nanoparticles are more suitable for the intracellular magnetic labeling<sup>17</sup>; however, the higher surface-to-volume ratio of nanoparticles leads to lower encapsulation efficiency and a faster rate of degradation, resulting in higher iron content loss after the same amount of time.<sup>16</sup> On the other hand, microparticles have higher encapsulation efficiency and a more delayed and attenuated aggregation peak.<sup>16</sup> In order to prepare IONPs encapsulated PLGA microparticles and nanoparticles, different experimental setups were employed in their study: microparticles (~2 μm) were fabricated by oil-in-water (O/W) emulsion using homogenization, while nanoparticles (~105 nm) were obtained via tip sonication induced O/W emulsion.<sup>16</sup> Second, due to the hydrophobic nature of PLGA, this method is limited to encapsulating hydrophobic IONPs.

For the purpose of extending the application of IONPs for targeted therapy and *in vivo* diagnosis, encapsulation of hydrophilic IONPs is necessary. Because IONPs must have a good dispersion in the aqueous environment.<sup>18</sup> And a hydrophilic surface of the IONPs can increase its circulatory half-life in the blood stream from minutes to hours or days.<sup>7</sup> Typically, the encapsulation of hydrophilic IONPs into hydrophobic polymer particles is carried out by a conventional W/O/W double emulsion method, in which IONPs sit in the inner water phase.<sup>19</sup> But it has some significant drawbacks to scale up for industrial production. First, it takes two steps for emulsion formation: an internal W/O emulsion, then an O/W emulsion; Second, it mostly generates only micron-/submicron-sized particles (>200 nm) rather than nanoparticles (50–200 nm).<sup>20</sup> Last, with the existence of internal water phase, no solid spheres are generated as the hydrophilic IONPs carriers.<sup>21</sup> This reduces the capability for designing particles tailored toward different release behaviors.

In this study, PLA particles encapsulating IONPs were produced using a fast (~2 min emulsion) and adaptable one-step W/O/W emulsion method under a viscous turbulent shear flow, controlled by the addition of glycerol into the aqueous continuous phase. This method makes it possible the preparation of either micron-sized or nano-sized PLA particles encapsulated with either hydrophobic or hydrophilic IONPs, through the adjustment of the viscosity of water phase and emulsification temperature. PLA nanospheres (~80 nm) with hydrophilic IONPs were generated via the dynamic HT-RT emulsion, processed initially under high temperature (HT, 60 °C) condition and then at room temperature (RT, 25 °C). Given the simplicity and short processing time, this method can present a commercially viable solution to a successful scale-up.

## EXPERIMENTAL

### Materials

Iron (II) chloride tetrahydrate ( $\text{FeCl}_2 \cdot 4\text{H}_2\text{O}$ ) (Reagent grade 99%), iron (III) chloride ( $\text{FeCl}_3$ ) (Reagent grade 97%), oleic acid (analytical standard) and Pluronic F68 (PF68) (average  $M_w = 8,400$  Da) were purchased from Sigma Aldrich. Citric acid monohydrate powder was purchased from Fisher Scientific Co. Poly (D,L-lactic acid) ( $M_w = 51,000$  Da,  $T_g = 52.5$  °C) was obtained from LakeShore Biomaterials. Ethyl acetate (EA), glycerol, and ammonium hydroxide ( $\text{NH}_4\text{OH}$ ) were purchased from J.T. BAKER and used as received. Deionized (DI) water used in all the process was supplied by a Barnstead nanopure Diamond-UV purification unit equipped with a UV source and final 0.2- $\mu\text{m}$  filter at 18.2 M $\Omega$  purity.

### Experiments

**Preparation of Hydrophilic and Hydrophobic IONPs.** Hydrophilic IONPs ( $\text{Fe}_2\text{O}_3$ ) used in the study were prepared following the method suggested in the previous study.<sup>22,23</sup> Briefly speaking, the mixture of  $\text{Fe}^{2+}$  and  $\text{Fe}^{3+}$  (1:2 molar ratio) with 40 mL water was heated to 80 °C under nitrogen purging. 5 mL  $\text{NH}_4\text{OH}$  was introduced by syringe while maintaining the temperature of the mixture at 80 °C for another 30 min. About 1 mL citric acid (CA) (2.38M) was added to the mixture and the temperature was raised to 95 °C. Heating is continued for

another 90 min. IONPs were cooled, separated, and washed with a mixture of acetone and water three times by centrifugation. The IONPs were dispersed in DI water and stored at room temperature for use.

Hydrophobic IONPs were prepared in the same way, except using oleic acid (0.15 mL) in place of citric acid for a hydrophobic coating. The resulting IONPs were washed with a mixture of hexane and acetone (1:1) for three times to obtain stable IONPs colloid. The purified suspension was then dispersed into hexane for storage.

**Preparation of Hydrophilic/Hydrophobic IONPs Encapsulated PLA Particles.** EA and DI water were mutually saturated before being used for emulsion experiment. PLA solution (oil phase) was prepared by dissolving 15 mg/mL PLA into water-saturated EA. Aqueous solution (water phase) was prepared by dissolving 15 mg/mL PF68 in the EA-saturated water/glycerol (50% v/v) system. For the encapsulation of hydrophobic IONPs, IONPs were dispersed into the oil phase. For hydrophilic IONPs, IONPs were dispersed into the water phase. Totally, 6 mL oil phase was emulsified with 18 mL water phase using Nanomixer at the speed of 12,500  $\text{s}^{-1}$  for 2 min under HT or RT, by controlling the cooling system circulating around the Nanomixer tank. The resulting emulsion was then poured into 90 mL pure DI water to induce the diffusion of EA and the solidification of polymer particles. The final colloid dispersion after overnight diffusion was transferred to glass vial and used for further characterization.

**Scanning and Transmission Electron Microscopies.** Scanning Electron Microscope (SEM) (JEOL 7500F) was used to observe particles morphology. The polymer particles dispersion was filtered using 0.1 $\mu\text{m}$  or 0.03 $\mu\text{m}$  pore size filter paper, air dried, and sputter coated with platinum for the SEM characterization. SEM images were taken under 3kV electron accelerating voltage, ~4.5 mm working distance. Transmission electron microscopy (TEM) (JEOL 2200FS) was carried out to observe the distribution of magnetic NPs in the polymer matrix. Freeze-drying microparticles were embedded into resin and then microtomed to give the cross-sectional view. For nanoparticles, the particle suspension was moved into a dialysis membrane tube, under a slow stirring water bath to gently remove glycerol and excessive surfactant PF68. After 3 days of dialysis, the suspension was then diluted 1:10 with DI water. Then several drops of the dilution were dripped on the carbon coated copper grid and air dried.

**Particle Size Distribution.** The particle size was measured using ImageJ from randomly collecting the diameter of a large number (300 each) of particles from the SEM images. The mean particle size and standard deviation were obtained directly from ImageJ. The histogram was plotted with a 30 nm bin from 0 to 300 nm.

**Zeta Potential Measurement.** ZetaPALS (Brookhaven Instruments Corporation) was employed to measure surface charge of particles. The electrode was conditioned to reach 13,200 mV of conductance with 1.5 mL sodium chloride (NaCl) solution (0.9 wt/vol %). Particles suspension was diluted to 1:10 with the

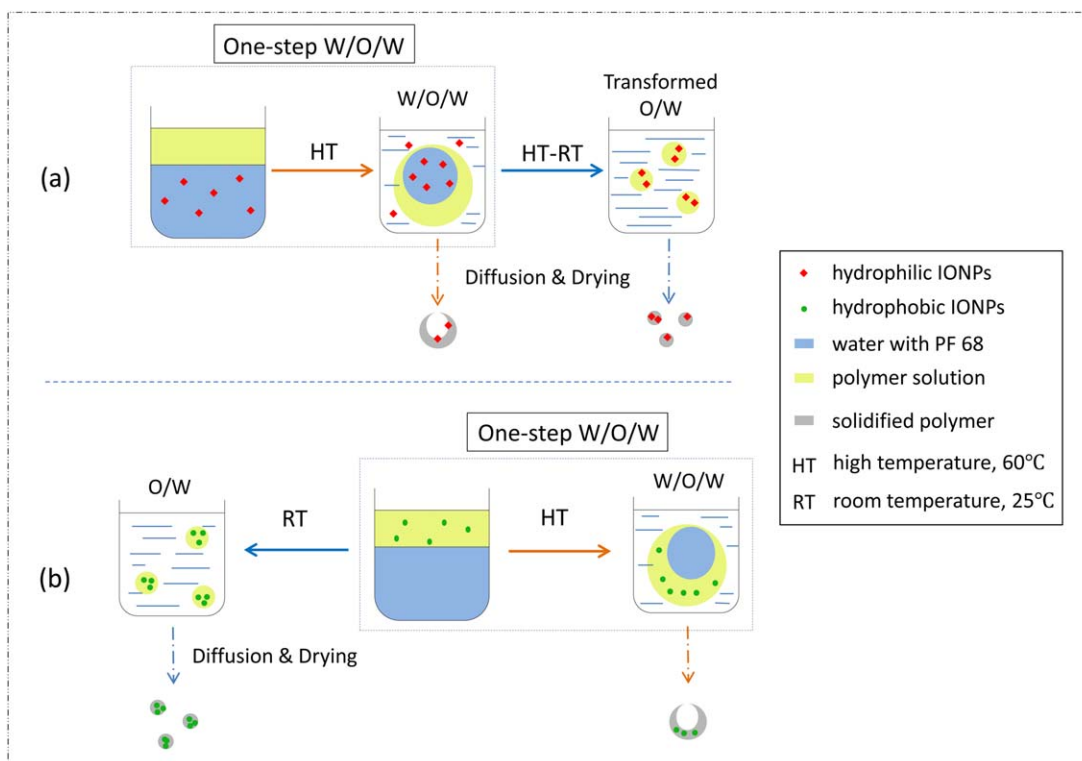


**Figure 1.** Schematic preparation procedures of (a) PLA-hydrophilic IONPs micro-/nano-particles, (b) PLA-hydrophobic IONPs micro-/nano-particles. [Color figure can be viewed in the online issue, which is available at [wileyonlinelibrary.com](http://wileyonlinelibrary.com).]

NaCl solution. In order to get a reliable data, each sample was subjected to 10 runs, and each run was composed of 30 cycles.

## RESULTS AND DISCUSSION

### One-Step W/O/W-Emulsion Formation Method

Figure 1 describes the overall schematic encapsulation methods and procedures used in this work. Figure 1(a) demonstrates the encapsulation of hydrophilic IONPs into PLA particles via our one-step W/O/W emulsion. The W/O/W double emulsion is widely used to encapsulate hydrophilic substances into hydrophobic polymer particles.<sup>24,25</sup> Conventionally, to form a W/O/W emulsion, two sequential emulsion processes are used with usually different recipes of inner and outer water phases.<sup>21</sup> The complexity of this method limits the loading efficiency and thus decreases the commercial scale-up possibility in the pharmaceutical industry. To produce polymeric particles encapsulating hydrophilic particles, the procedure of W/O/W emulsion needs to be simplified. In our previous study, a novel, one-step W/O/W-emulsion formation method was developed via a modified Taylor-Couette mixer.<sup>26</sup> Compared to the conventional two-step W/O/W formation, the present method significantly reduced the particles preparation duration time and simplified process. The modified Taylor-Couette mixer used in this study, also called Nanomixer, consists of two concentric cylinders with the inner perforated turbine and the outer cylindrical vessel. The gap between two cylinders is  $\sim 2$  mm and thus generates a high shear force in the closed vessel, leading to a turbulent fluid flow mixing condition. Under turbulent condition, the dispersed emulsion droplets may undergo deformation, breakup or coales-

cence upon the action of viscous or inertial stress. The dominant stress in the flow is determined by the size of the smallest turbulent eddies,  $\lambda$ . When  $\lambda$  is smaller than the initial droplet size, the mixing condition is inertial turbulent regime; when  $\lambda$  is larger than the maximum initial droplet size, the mixing is under viscous turbulent regime. According to “Kolmogorov Scale”,<sup>27</sup> the eddy diameter is proportional to the viscosity of the continuous phase. In this study, the viscosity of continuous phase was controlled by adding different volume fractions of glycerol into the water phase while the overall ratio of oil phase to water phase fixed at 1:3. This was discussed in detail in our previous study where the eddy size increased with the increasing amount of glycerol.<sup>1</sup> The results showed that the eddy size was larger than the maximum initial droplet size when the fraction of glycerol was beyond  $\sim 40\%$  (v/v). When the water phase contained 40% (v/v) glycerol or less (viscosity  $\sim 1.5$  cP), solid nanospheres were obtained, suggesting the formation of O/W single emulsion in which oil droplets containing PLA were dispersed. When 50% (v/v) or more glycerol was applied, open-hollow microparticles were formed, which implied the formation of W/O/W double emulsion [Figure 1(a), HT]. Therefore, under the same emulsification temperature (HT, 60 °C), the transitional behavior between O/W emulsion and W/O/W emulsion were dependent on the viscosity of continuous phase.<sup>26</sup> In addition to viscosity, emulsification temperature was another key factor in the formation of one-step W/O/W emulsion. When the temperature was greater than its glass transition temperature ( $T_{g,PLA} = 52$  °C), the mobility of PLA chain segments greatly increased and thus droplets tended to be deformed and

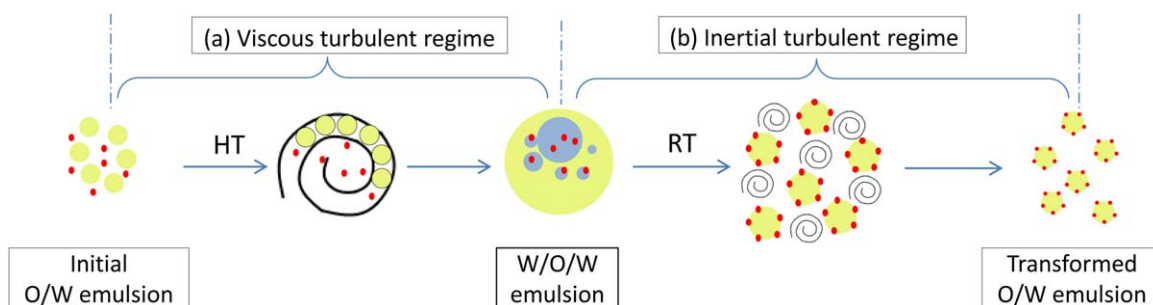


**Figure 2.** Schematic mechanism of encapsulating hydrophilic IONPs into PLA particles. [Color figure can be viewed in the online issue, which is available at [wileyonlinelibrary.com](http://wileyonlinelibrary.com).]

elongated which increased the coalescence among multi-body collisions. The chosen 60 °C is between the glass transition temperature of PLA and the boiling point of ethyl acetate (77 °C). In summary, the HT condition and the change in viscosity resulted in a viscous turbulent regime. The sizes of eddies formed were larger than the initial O/W droplets. When droplets were caught inside a large-size eddy, O/W droplets engaged with collision and coalescence to form W/O/W double emulsion droplets [Figure 2(a)]. This process is considered the one-step W/O/W emulsion [adaptable emulsion, Figure 1(a)] method in this study. When the emulsification temperature was reduced to room temperature (RT), the mixing condition changed back to the inertial turbulent flow, in which the eddy size was smaller than the droplet size. Thus, large-size W/O/W droplets were broken up into small O/W droplets by shear force [Figure 2(b)]<sup>28</sup> and this resulted in the formation of nanoparticles [Figure 1(a), HT-RT].

Meanwhile, in the case of hydrophobic IONPs, the emulsification at HT generated open-hollow microparticles in the same way as hydrophilic IONPs [Figure 1(b)]. At RT, nanoparticles with hydrophobic IONPs were generated based on the typical O/W emulsion as shown in Figure 1(b). In this work, the percentage of glycerol was fixed at 50% (v/v) in order to control the emulsion droplet transformation between W/O/W and O/W only by emulsification temperature (Figure 1). Then, micro- and nano-polymeric particles incorporating IONPs were generated under HT and RT, respectively.

### Generation of PLA-Hydrophilic IONPs Micron-/Nano-Sized Particles

Based on the preparation method mentioned in the previous section, polymeric (PLA) particles encapsulating hydrophilic IONPs were prepared under different emulsification temperature conditions (Table I), resulting in particles of different shapes and sizes. For comparison, PLA particles without IONPs were generated [Figure 3(a,b)]. At HT, PLA particles with open-hollow structure were generated (Sample A, Table I) as shown in Figure 3(a). The hollow structure resulting from the drying of the inner water phase of W/O/W droplet is as shown in Figure 1(a). The opening of particles was caused by polymer solidification during the solvent diffusion process. During the diffusion of solvent (ethyl acetate), spherical W/O/W emulsion droplets shrunk to smaller size. When the droplet size was close enough to the inner water bubble size, polymer content was not sufficient to form a resistant layer around the incompressible inner water phase.<sup>21</sup> PLA nanoparticles (Sample B, Table I) were obtained at HT-RT due to the transformation of W/O/W emulsion to O/W emulsion. The nanoparticles were solid and spherical as shown in Figure 3(b).

PLA-hydrophilic IONPs microparticles and nanoparticles were obtained by the process shown in Figure 1(a) and Figure 2, in which hydrophilic IONPs were initially dispersed in water phase. Composite microparticles [Figure 3(c,e)] were obtained from W/O/W emulsion in HT step followed by diffusion-drying process. As shown in Figure 3(c), compared to pure PLA

**Table I.** Emulsion Conditions of PLA and PLA-IONPs Particles

Sample no.	Particle composition	Preparation parameters			
		$C_{PLA}$ (mg/mL)	IONPs location	Glycerol (% v/v)	Emulsion temp.
A	PLA MP <sup>a</sup>	15	N	50	HT
B	PLA NP <sup>b</sup>	15	N	50	HT-RT
C	PLA-hydrophilic IONPs MP	15	Water phase	50	HT
D	PLA-hydrophilic IONPs NP	15	Water phase	50	HT-RT
E	PLA-hydrophobic IONPs MP	15	Oil phase	50	HT
F	PLA-hydrophobic IONPs NP	15	Oil phase	50	RT
G	PLA-hydrophobic IONPs NP	15	Oil phase	0	RT

<sup>a</sup> Microparticle.

<sup>b</sup> Nanoparticle.

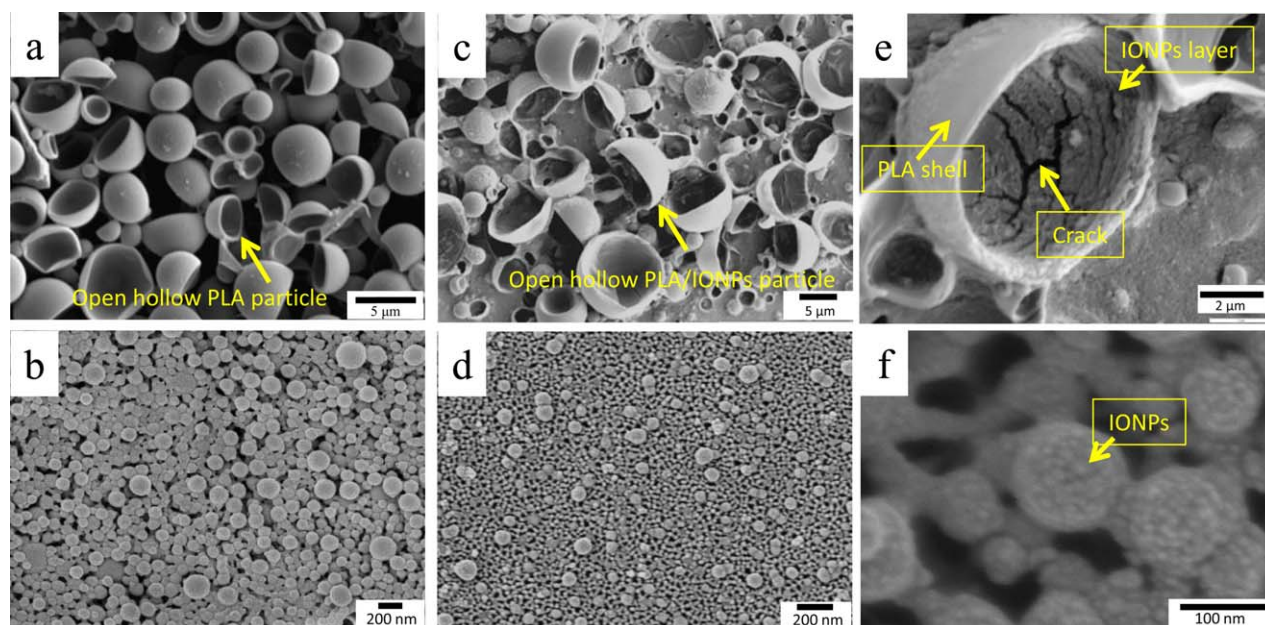


**Figure 3.** SEM images of (a) PLA microparticles - Sample A, (b) PLA nanoparticles - Sample B, (c,e) PLA-hydrophilic IONPs microparticles - Sample C, (d,f) PLA-hydrophilic IONPs nanoparticles - Sample D. [Color figure can be viewed in the online issue, which is available at [wileyonlinelibrary.com](http://wileyonlinelibrary.com).]

microparticles, the addition of hydrophilic IONPs did not change the open-hollow structure and the overall particle size distribution ( $\sim 5 \mu\text{m}$ ). This is because the hydrophilic IONPs could not go into the oil phase and thus do not affect the polymer phase concentration. In the formation of W/O/W emulsion droplets, most hydrophilic IONPs were sitting in the inner water phase and were trapped into particle shell during the diffusion and drying process [Figure 1(a)]. During the solvent diffusion process, PLA was gradually precipitated around the inner water droplet, forming the shell of capsule-structure particle. The hydrophilic IONPs were retained on the shrinking polymer shell when the inner water phase transferred across the dynamic solidifying polymer shell of the micro-sized particles.<sup>29</sup> PLA shell formed a hydrophobic wall to retard the leakage of hydrophilic IONPs into the outer water phase. When applying higher magnification on the individual composite particle [Figure 3(e)], NPs ( $\sim 10\text{nm}$ ) were observed on both the inner and outer surface of PLA particle. The inner particle surface was rougher than the outer, with the appearance of cracks. It has been reported that the magnetic NPs at the interface could induce the buckling instability of emulsion droplets during the solvent removal, causing the shrinkage of particles.<sup>30</sup> This is consistent with our proposed W/O/W emulsion formation, namely, hydrophilic IONPs have been captured into the inner water phase (Figure 2).

PLA-hydrophilic IONPs nanoparticles [Figure 3(d,f)] were prepared via a HT followed by RT (HT-RT) step [Figure 1(a)]. That is, the W/O/W emulsion was emulsified again under the room temperature (RT emulsion). As shown in Figure 2, when a RT emulsion step was carried out after the HT emulsion step, the W/O/W droplets might undergo deformation by the small-sized eddies. Under deformation, breakup and coalescence of the droplets occurred competitively, turning W/O/W droplets

into single emulsion (O/W) droplets. The flow-induced deformation promoted the interaction between the inner and outer interfaces, enhancing the entrapment of hydrophilic IONPs inside droplets.<sup>25</sup> During this process, IONPs stayed more on the outside of the oil droplet. The SEM image of higher magnification [Figure 3(f)] demonstrates individually distributed NPs ( $\sim 10\text{nm}$ ) on the PLA particle surface. Most PLA particles were covered with IONPs like a “raspberry”. Compared with the limited previous study on hydrophilic IONPs encapsulated polymeric particles,<sup>19,31,32</sup> the particles prepared by our method showed a denser encapsulation of IONPs. In addition, IONPs distribute more uniformly in our method.<sup>19</sup>

In order to confirm the successful encapsulation of hydrophilic IONPs into PLA particles, TEM was applied to PLA-hydrophilic IONPs composite microparticles and nanoparticles (Figure 4). Figure 4(a) shows a black (embedded IONPs) open-ring structure, which is consistent with our SEM observation of open-hollow microparticles [Figure 3(c,e)]. The higher magnification TEM image [Figure 4(b)] provides details of the local region of this microparticle. The thickness of the black region was  $\sim 120\text{nm}$ , which was composed of IONPs with  $\sim 10\text{nm}$  in diameter while the thickness of PLA/IONPs particle shell from the SEM image [Figure 3(e)] was about  $150\text{nm}$ . As shown in Figure 4(a), the inner particle surface was relatively smooth, which suggests that IONPs were mostly embedded within the PLA shell, with few sitting on the inner surface. The IONPs seemed individually distributed, aggregate with each other and densely stacked along the length of PLA shell. Figure 4(c,d) demonstrates the stacking entrapment of hydrophilic IONPs inside the PLA nanoparticles. Nanoparticles were not homogeneously spherical [Figure 4(c)], suggesting that IONPs locate more on particle surfaces as shown in the SEM observation [Figure 3(f)].

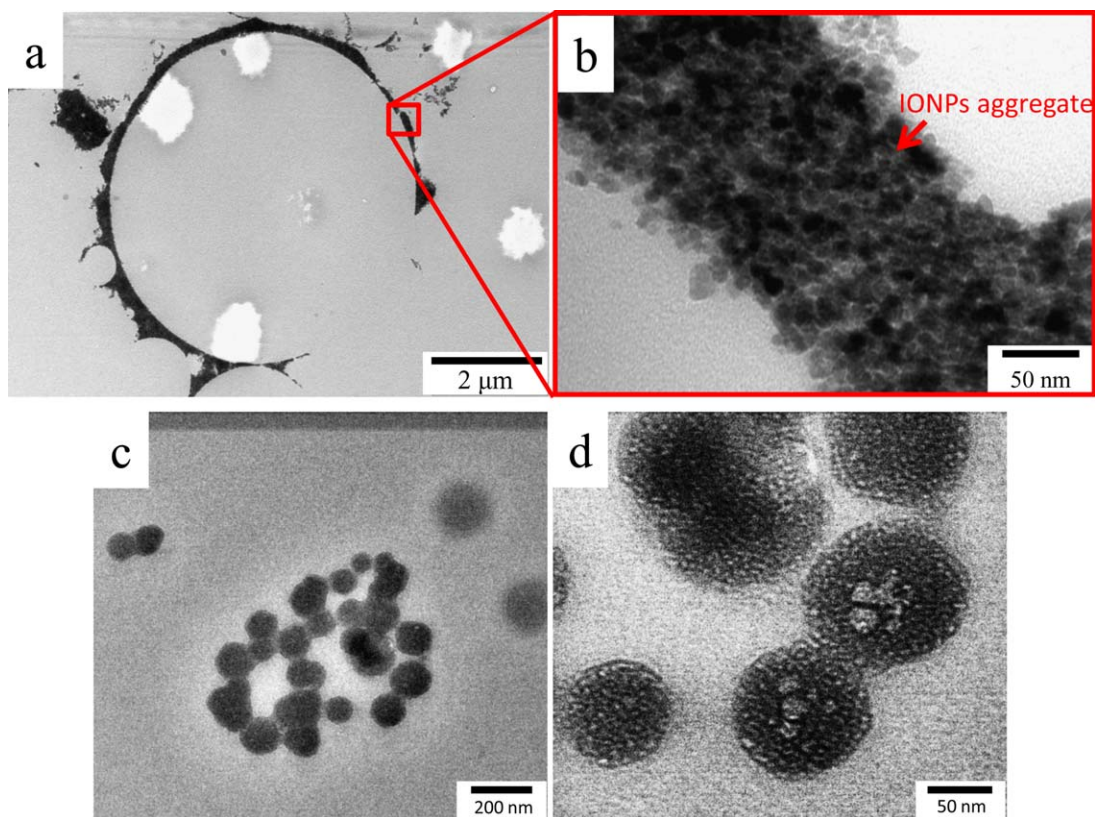


**Figure 4.** TEM images of (a,b) PLA-hydrophilic IONPs hollow microparticles, (c,d) PLA-hydrophilic IONPs nanospheres. [Color figure can be viewed in the online issue, which is available at [wileyonlinelibrary.com](http://wileyonlinelibrary.com).]

To test the magnetic performance of microparticles with hydrophilic IONPs, the resulting particle suspension was collected into a vessel and set next to a magnetic bar. PLA-hydrophilic

IONPs composite microparticles slowly moved towards the magnet bar (less than 15 min) as shown in Figure 5. Meanwhile, the particle suspension became transparent, which suggests a



**Figure 5.** Migration of PLA-hydrophilic IONPs composite particles under the magnetic field by a magnet; before (left) and after (right). [Color figure can be viewed in the online issue, which is available at [wileyonlinelibrary.com](http://wileyonlinelibrary.com).]

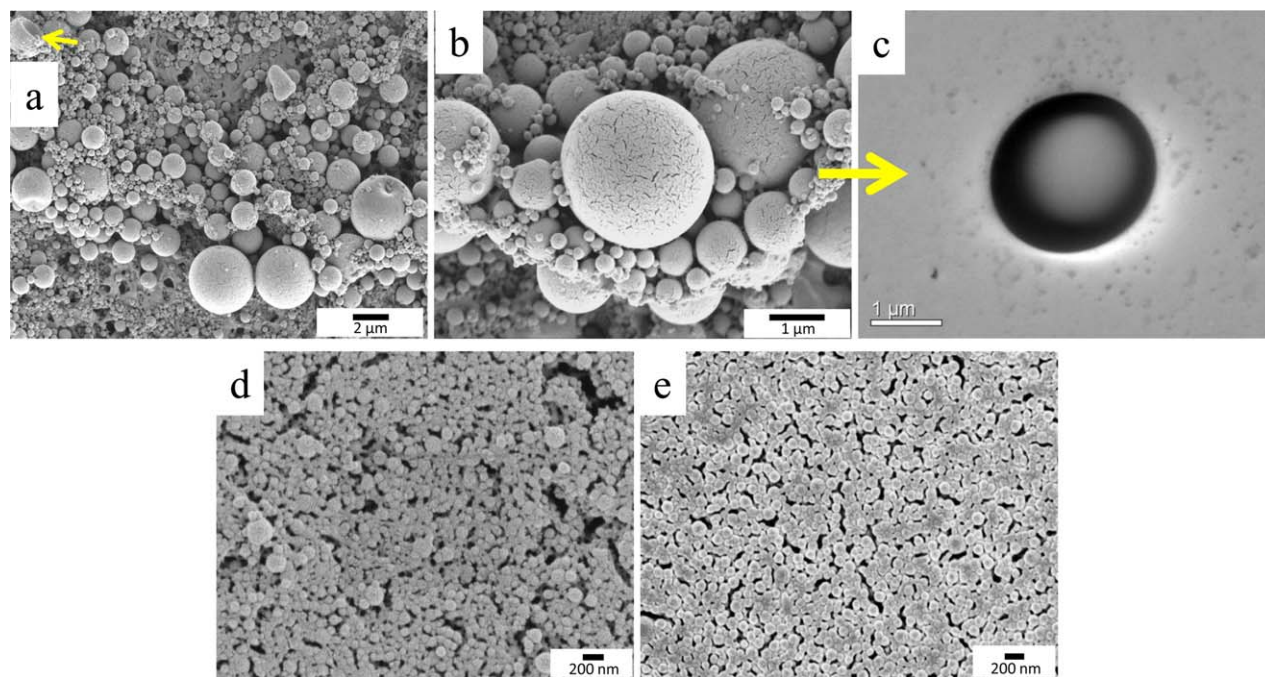


**Figure 6.** (a,b) SEM images of PLA-hydrophobic IONPs microparticles - Sample E, (c) TEM image of PLA-hydrophobic IONPs microparticle - Sample E, (d) SEM image of PLA-hydrophobic IONPs nanoparticles - Sample F (with glycerol), (e) SEM image of PLA-hydrophobic IONPs nanoparticles - Sample G (without glycerol). [Color figure can be viewed in the online issue, which is available at [wileyonlinelibrary.com](http://wileyonlinelibrary.com).]

high loading efficiency of hydrophilic IONPs into PLA microparticles.

#### Generation of PLA-Hydrophobic IONPs Micron-/Nano-Sized Particles

The PLA-hydrophobic IONPs micron-/nano-particles were prepared via the process shown in Figure 1(b). The SEM results (Figure 6) show the morphology of samples E-G from Table I. Figure 6(a-c) shows that the addition of hydrophobic IONPs significantly changed the microparticle structure and size. Compared with the plain PLA and PLA-hydrophilic IONPs composite particles, PLA-hydrophobic IONPs particles have a closed microparticle structure and smaller mean particle size ( $\sim 2 \mu\text{m}$ ) [Figure 6(a)]. This is probably because hydrophilic IONPs were added into the water phase while hydrophobic ones were added into the oil phase which dissolved PLA. Therefore, during the solvent diffusion process, the PLA-hydrophobic IONPs particles maintained a spherical shape because the concentration of the oil phase (polymer plus hydrophobic IONPs) was high enough to form a resistant layer around the inner water droplet.<sup>21</sup> This led to the formation of the closed-hollow microparticles after drying [Figure 6(c)]. IONPs-induced anisotropic shrinkage<sup>30</sup> caused cracks on the surface or collapse of polymer particles as shown in a higher magnification [Figure 6(b)]. To encapsulate hydrophobic IONPs into PLA nanoparticles, the one-step W/O/W emulsion was not necessary and RT was enough to capture hydrophobic IONPs [Figure 1(b), RT], corresponding to sample F in Table I [Figure 6(d)]. As comparison, a conventional O/W single emulsion, without glycerol in the water phase, was carried out [Figure 6(e)].

Figure 7 shows the TEM images of sample F and G. In Figure 7(a,b), which represent PLA/hydrophobic IONPs nanoparticles with 50% (v/v) glycerol (Sample F), the hydrophobic IONPs sit more on the edge of the particle rather than in the middle. On the other hand, in Figure 7(c,d) (Sample G), the concentration of IONPs was denser in the middle than in the particle edge. To confirm such a difference in the location of IONPs, the surface property was measured using the zeta potential (Table II). The surface charge of pure PLA particle is  $-10.18 \text{ mV}$ . Hydrophobic IONPs used in this study is anionic resulting from the oleic acid coating. Nanoparticles prepared with glycerol (Sample F) showed a larger absolute zeta potential value than the one without glycerol (Sample G), which was consistent with the TEM observation. The reason might be that the diffusion of solvent for sample F is slower because of the existence of glycerol in the outer water phase. The motion of IONPs was mainly driven by the diffusion of ethyl acetate towards the outer water phase. In Sample F, the addition of glycerol increased the viscosity of the outer water phase and thus hindered the diffusion, leading to a slower movement of IONPs along the diffusion direction. This feature can be used to tailor the distribution and thus the release behavior of IONPs. In addition, further slowing down the diffusion process may increase the zeta potential of PLA particles and thus improve the colloidal stability.<sup>33</sup>

For polymeric particles with hydrophobic IONPs, no matter how the emulsion was generated (an o/w droplet or w/o/w droplet forms), the hydrophobic IONPs were encapsulated within the polymer matrix (Figure 6) and the particle size was controllable from micron-size to nano-size.

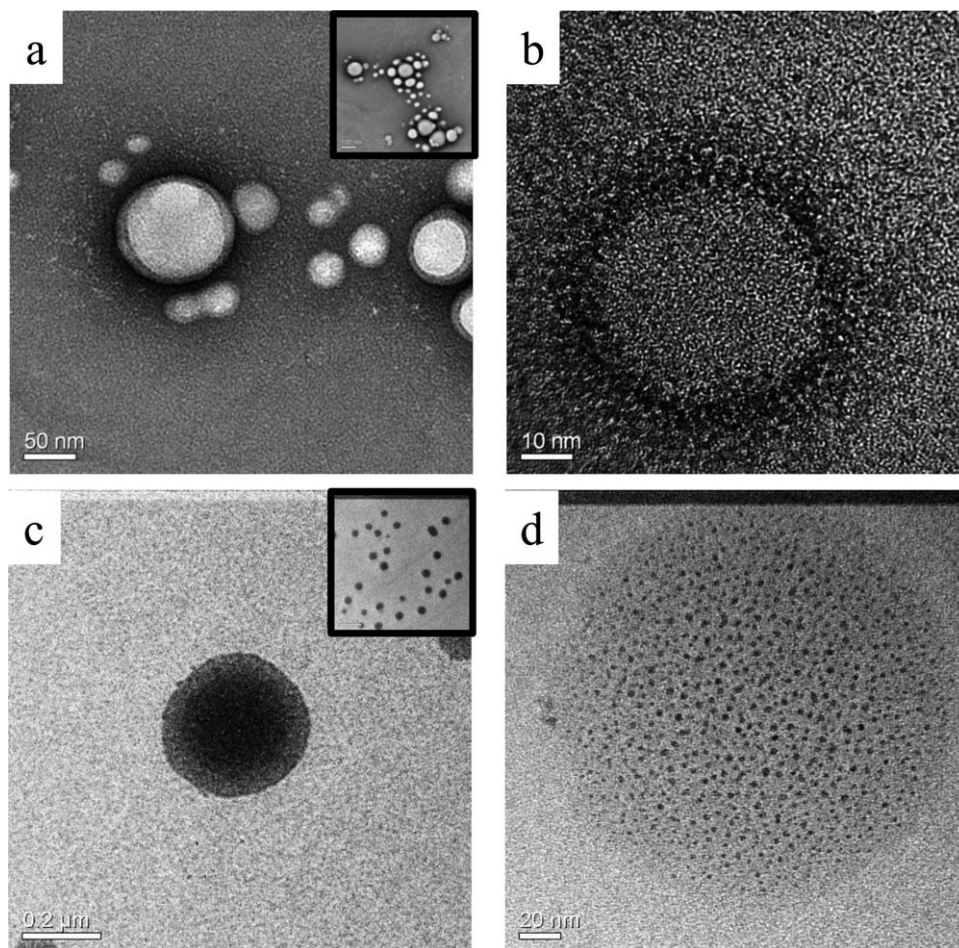


**Figure 7.** TEM images of PLA-hydrophobic IONPs composite nanoparticles (a,b) prepared with glycerol in Water phase - Sample F, (c,d) prepared without glycerol - Sample G. Black dots represent IONPs.

### Analysis of Particle Size

**Effect of Dynamic HT-RT Process on Particle Size.** From the previous results,<sup>26</sup> with the same experimental setup, pure PLA nanoparticles generated from HT-RT process ( $\sim 104$  nm) showed a smaller mean particle size than that from RT emulsion ( $\sim 164$  nm) [Figure 1(b)-RT]. On the other hand, PLA nanoparticles prepared from HT-RT process showed a higher polydispersity. This gives us a tool to reduce the size of nanoparticles: more repeated HT-RT processes lead to smaller particle size.

Our dynamic HT-RT process has the advantage in preparing composite nanoparticles which are better suited for cell labeling, since the NPs need to go through the cell membrane.<sup>17</sup> As shown in Figure 8(b), the obtained PLA-hydrophilic IONPs nanoparticles have a much lower average particle size ( $\sim 80$  nm) than that has been reported by literature ( $\sim 200$  nm).<sup>19,31</sup> From the diagram, we can see that 90% of the particles are within 100 nm with the minimum particle size is about 30 nm.

**Effect of IONPS on Particle Size.** For microparticles, the addition of hydrophilic IONPs in water phase did not significantly affect the composite particle shape and size while hydrophobic IONPs sitting in oil phase decreased the overall particle size and changed the particle to a closed-sphere shape. As mentioned

before, this is because hydrophobic IONPs increased the overall oil phase concentration. Thus, during the solvent diffusion process, polymer/IONPs formed a continuous layer and the diameter of a spherical particle was smaller than a hemisphere of the same volume. For nanoparticles, as shown in Fig. 8, the addition of IONPs, no matter hydrophilic or hydrophobic, decreased the composite particle size compared to pure PLA nanoparticles [Figure 3(b)]. The mean particle sizes of PLA-IONPs nanoparticles were about 20 nm smaller than that of pure PLA particles. The possible reason would be that the existence of IONPs resulted in Pickering emulsion (solids-stabilized emulsion).<sup>34</sup> Under the turbulent-inertial flow, droplets were stabilized by IONPs and thus kept as smaller droplets.

**Table II.** Zeta Potential (mV) of PLA-Hydrophobic IONPs Composite Nanoparticles

Samples	Zeta potential (mV)
Sample F	$-30.87 \pm 1.51$
Sample G	$-26.90 \pm 1.26$
Pure PLA NPs	$-10.18 \pm 1.19$

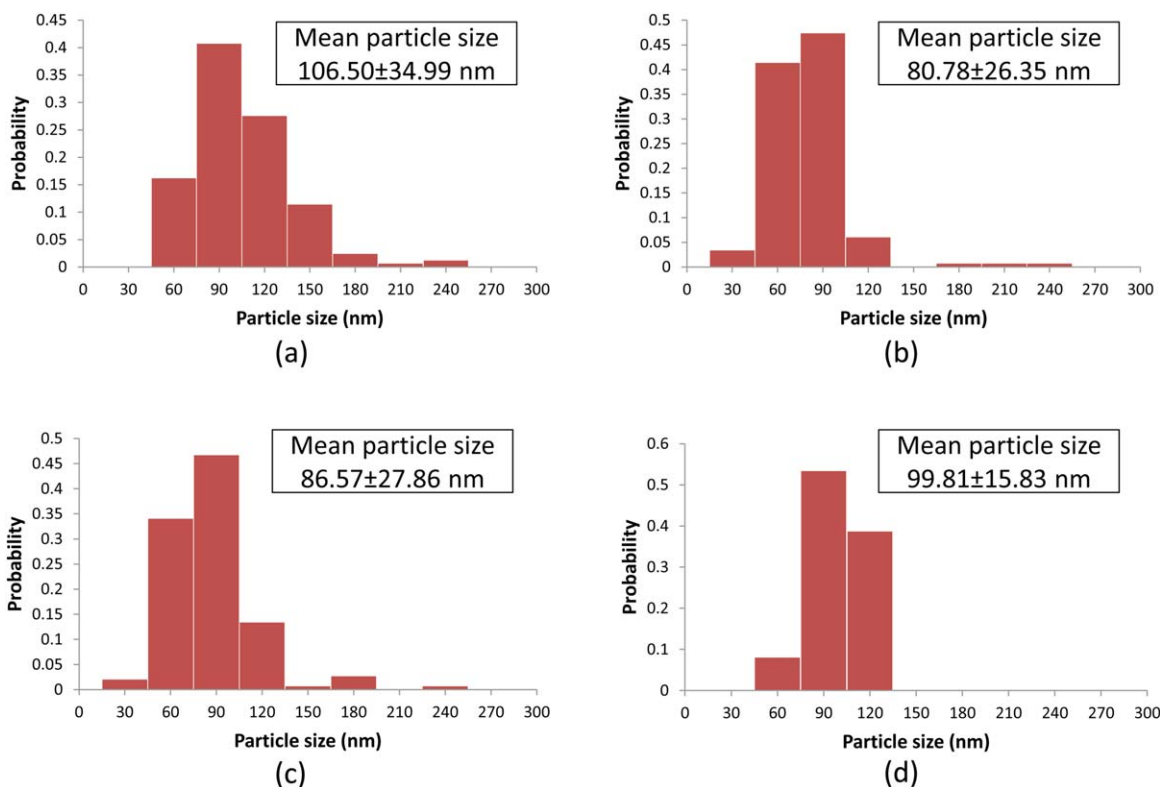


**Figure 8.** Particle size distributions. (a) plain PLA NPs - Sample B, (b) PLA-hydrophilic IONPs NPs - Sample D, (c) PLA-hydrophobic IONPs NPs - Sample F, (d) PLA-hydrophobic IONPs NPs - Sample G. [Color figure can be viewed in the online issue, which is available at [wileyonlinelibrary.com](http://wileyonlinelibrary.com).]

## CONCLUSIONS

Magnetic PLA microparticles and nanospheres were successfully prepared by a fast, one-step W/O/W emulsion method without introducing any surface coating or modification. The formation of multiple-emulsion droplets entrapping hydrophilic IONPs in the inner compartments as well as the diffusion of these NPs to the polymer matrix during the solvent removal and drying process played an important role in dispersing hydrophilic NPs in the hydrophobic polymer. The particle sizes and shapes were well controlled by operating different emulsion conditions. The SEM and TEM results revealed the well-dispersed IONPs in the polymer shell and sphere. The flexible encapsulation of hydrophobic and hydrophilic IONPs and controllable particle size preparation allow achieving different applications. This process can also be applied to prepare carriers of water soluble drugs or molecules of interest, e.g., penicillin and doxorubicin hydrochloride, with an improved compatibility of composite components. The facile and fast process operation sheds light on the potential scale-up production of biodegradable magnetic particles.

## ACKNOWLEDGMENTS

Authors greatly appreciate the funding from the Michigan Initiative for Innovation and Entrepreneurship and the MSU Foundation, and in part from the DOD Strategic Environmental Research and Development Program (DOD SERDP W912HQ-12-C-0020).

## REFERENCES

- Gupta, A. K.; Gupta, M. *Biomaterials* **2005**, *26*, 3995.
- Mornet, S. P.; Vasseur, S. b.; Grasset, F.; Duguet, E. *J. Mater. Chem.* **2004**, *14*, 2161.
- Susumu Taketomi, M. U.; Mizukami, M.; Miyajima, H.; Chikazumi, S. *J. Phys. Soc. Jpn.* **1987**, *56*, 3362.
- Tsang, S. C.; Caps, V. R.; Paraskevas, I.; Chadwick, D.; Thompson, D. *Angewandte Chemie* **2004**, *116*, 5763.
- Makoto Takafuji, S. I.; Ihara, H.; Xu, Z. *Chem. Mater.* **2004**, *16*, 1977.
- Daniel, W.; Elliott, W. X. *Z. Environ. Sci. Technol.* **2001**, *35*, 4922.
- Arruebo, M.; Fernandez-Pacheco, R.; Ibarra, M. R.; Santamaria, J. *Nano Today* **2007**, *2*, 22.
- Kenneth, J.; Widder, A. E. S.; Dante, G. *Scarpelli, Experimental Biology and Medicine* **1978**, *158*, 141.
- Shapiro, E. M. *Magn. Reson. Med.* **2015**, *73*, 376.
- Lu, A. H.; Salabas, E. L.; Schuth, F. *Angew Chem Int. Ed. Engl.* **2007**, *46*, 1222.
- Lu, Y.; Brian, Y. Y.; Mayers, T.; Xia, Y. *Nano Lett.* **2002**, *2*, 4.
- Bulte, J. W. M.; Kraitchman, D. L. *NMR Biomed.* **2004**, *17*, 484.
- Arbab, A. S. B.; Lindsey, A.; Miller, Bradley, R.; Jordan, Elaine, K.; Bulte, Jeff, W. M.; Frank, Joseph, A. *Transplantation* **2003**, *76*, 8.

14. Hinds, K. A.; Hill, J. M.; Shapiro, E. M.; Laukkanen, M. O.; Silva, A. C.; Combs, C. A.; Varney, T. R.; Balaban, R. S.; Koretsky, A. P.; Dunbar, C. E. *Blood* **2003**, *102*, 867.
15. Shapiro, E. M.; Skrtic, S.; Koretsky, A. P. *Magn. Reson. Med.* **2005**, *53*, 329.
16. Michael, K.; Nkansah, D. T.; Erik, M.; Shapiro, E. M. *Magn. Reson. Med.* **2011**, *65*, 10.
17. Bertorelle, F.; Wilhelm, C.; Roger, J.; Gazeau, F.; Menager, C.; Cabuil, V. *Langmuir* **2006**, *22*, 5385.
18. Sun Sheng-Nan, W. C.; Zan-Zan, Z.; Yang-Long, H.; Venkatraman, S. S.; Zhi-Chuan, X. *Chin. Phys. B.* **2014**, *23*, 2014.
19. Hong Zhao, J. G. A. U. O. H. *Biomagn. Res. Technol.* **2007**, *5*, 2.
20. Khoe, S.; Yaghoobian, M. *Eur. J. Med. Chem.* **2009**, *44*, 2392.
21. Rosca, I. D.; Watari, F.; Uo, M. *J. Control Release* **2004**, *99*, 271.
22. Liu, Z. L.; Wang, H. B.; Lu, Q. H.; Du, G. H.; Peng, L.; Du, Y. Q.; Zhang, S. M.; Yao, K. L. *J. Magnet. Mater.* **2004**, *283*, 258.
23. Gokhale, A. A.; Lu, J.; Lee, I. *J. Mol. Catalysis B: Enzymatic* **2013**, *90*, 76.
24. Cohen-Sela, E.; Chorny, M.; Koroukhov, N.; Danenberg, H. D.; Golomb, G. *J. Control Release* **2009**, *133*, 90.
25. Ji, S. W.; Lu, J.; Liu, Z. G.; Srivastava, D.; Song, A.; Liu, Y.; Lee, I. *J. Colloid Interf. Sci.* **2014**, *423*, 85.
26. Ji, S.; Srivastava, D.; Parker, N. J.; Lee, I. *Polymer* **2012**, *53*, 205.
27. Boxall, J. A.; Koh, C. A.; Sloan, E. D.; Sum, A. K.; Wu, D. T. *Langmuir* **2012**, *28*, 104.
28. Stroeve, P.; Varanasi, P. P. *J. Colloid Interf. Sci.* **1984**, *99*, 360.
29. Wang, J.; Schwendeman, S. P. *J. Pharma. Sci.* **1999**, *88*, 1090.
30. Liu, B.; de Folter, J. W. J.; Möhwald, H. *Soft Matter* **2011**, *7*, 3744.
31. Vilos, C.; Gutierrez, M.; Escobar, R. A.; Morales, F.; Denardin, J. C.; Velasquez, L.; Altbir, D. *Electron J. Biotechnol.* **2013**, *16*.
32. Zhao, H.; Saatchi, K.; Hafeli, U. O. *J. Magn. Mater.* **2009**, *321*, 1356.
33. Hunter, R. J. *Zeta Potential in Colloid Science: Principles and Applications*; Academic Press, **2013**.
34. Xiao, Q.; Tan, X. K.; Ji, L. L.; Xue, J. *Synthetic Met.* **2007**, *157*, 784.